

PAPER • OPEN ACCESS

Cooling microwave fields into general multimode Gaussian states

To cite this article: Nahid Yazdi *et al* 2023 *New J. Phys.* **25** 083052

View the [article online](#) for updates and enhancements.

You may also like

- [Test of the statistical isotropy of the universe using gravitational waves](#)
Giacomo Galloni, Nicola Bartolo, Sabino Matarrese et al.
- [CMOS Compatible Growth of High Quality Ge, SiGe and SiGeSn for Photonic Device Applications](#)
Murtadha A. Alher, Aboozar Mosleh, Larry Cousar et al.
- [Charged black hole in 4D Einstein-Gauss-Bonnet gravity: particle motion, plasma effect on weak gravitational lensing and centre-of-mass energy](#)
Farruh Atamurotov, Sanjar Shaymatov, Pankaj Sheoran et al.



PAPER

Cooling microwave fields into general multimode Gaussian statesNahid Yazdi^{1,2}, Juan José García-Ripoll³ , Diego Porras³  and Carlos Navarrete-Benlloch^{2,4,5,*}¹ Department of Physics, Isfahan University of Technology, Isfahan 84156-83111, Iran² Wilczek Quantum Center, School of Physics and Astronomy, Shanghai Jiao Tong University, Shanghai 200240, People's Republic of China³ Institute of Fundamental Physics IFF-CSIC, Calle Serrano 113b, 28006 Madrid, Spain⁴ Max-Planck Institute for the Science of Light, Staudtstrasse 2, 91058 Erlangen, Germany⁵ Shanghai Research Center for Quantum Sciences, Shanghai 201315, People's Republic of China

* Author to whom any correspondence should be addressed.

E-mail: derekkorg@gmail.com**Keywords:** dissipative state preparation, superconducting circuits, multimode quantum information, quantum optics

RECEIVED

1 February 2023

REVISED

23 July 2023

ACCEPTED FOR PUBLICATION

16 August 2023

PUBLISHED

31 August 2023

Original Content from
this work may be used
under the terms of the
[Creative Commons
Attribution 4.0 licence](https://creativecommons.org/licenses/by/4.0/).

Any further distribution
of this work must
maintain attribution to
the author(s) and the title
of the work, journal
citation and DOI.

**Abstract**

We show that a collection of lossy multichromatic modulated qubits can be used to dissipatively engineer arbitrary Gaussian states of a set of bosonic modes. Our ideas are especially suited to superconducting-circuit architectures, where all the required ingredients are experimentally available. The generation of such multimode Gaussian states is necessary for many applications, most notably measurement-based quantum computation. We build upon some of our previous proposals, where we showed how to generate single-mode and two-mode squeezed states through cooling and lasing. Special care must be taken when extending these proposals to many bosonic modes, and we discuss here how to overcome all the limitations and hurdles that naturally appear. For the sake of illustration, we work out two examples of Gaussian-state families consisting of Greenberger–Horne–Zelinger and cluster states, which allow us to show that it is possible to use a set of N lossy qubits to cool down a bosonic chain of N modes to any desired Gaussian state.

1. Introduction

The generation of complex quantum states of many optical modes has been on the roadmap of quantum optics for quite some time [1]. Apart from their fundamental motivation on questions of entanglement [2], such states are necessary for technological applications such as measurement-based quantum computation [3–5]. Tremendous developments have been possible in this area thanks to nonlinear optical cavities [6–14], making photonic systems among the most serious contenders for large scale quantum information processing. Also serious contenders are devices based on superconducting circuits [15–17], where indeed the most advanced quantum computer prototypes are currently implemented [18–21]. In contrast to photonic systems, the generation of multimode bosonic states is still at its infancy on these platforms, so it is interesting to propose ways to generate such states exploiting the unique properties of superconducting circuits: low characteristic frequencies, on the GHz domain, and large effective dipole moments, conferring them strong nonlinearities that led to dubbing them ‘giant’ artificial atoms. These properties have allowed access to regimes that remained largely unexplored with other experimental platforms, for example, the ultra-strong coupling regime of light–matter interactions [22–25].

Exploiting the low characteristic frequencies of these systems, in this work we put forward a proposal for the generation of general multimode Gaussian states of microwave fields. Our scheme relies on the ability to modulate parameters of superconducting circuits at rates comparable to their natural energy scales [26, 27]. In fact, in previous works we have used similar ideas to show that squeezed states of microwave fields can be generated through cooling [28] or lasing [29], but restricted there to single-mode or two-mode Gaussian states. In the present work, we examine the possibility of using similar protocols to generate arbitrary Gaussian states of as many modes as one wants. We provide a positive answer, but not without several subtleties that impose nontrivial conditions that are necessary to examine in detail. From a more general

point of view, we study how to modulate a set of lossy qubits to dissipatively engineer arbitrary Gaussian states of a bosonic chain.

The article is structured as follows. In the next section we introduce the characterization of multimode Gaussian states, and present the core of our scheme that uses lossy qubits to cool down the bosonic modes to the desired Gaussian state. In section 3 we develop the protocol formally and discuss some potential limitations that were not present for single-mode or two-mode states. In sections 4 and 5 we work out detailed examples: the generation of cluster and Greenberger–Horne–Zeilinger (GHZ) states. With the examples at hand, section 6 is devoted to proving that the limitations mentioned before do not spoil our proposal. Throughout the article and for the sake of clarity in the presentation, our scheme is presented via a model in which all qubits are coupled to all bosonic modes; since this might be highly impractical, in section 7 we propose alternative models with local couplings only, which allow implementing our ideas as well. We finish the article in section 8 where we offer some conclusions and comment on how to extend our methods to generate multimode nonclassical lasing.

2. Multimode Gaussian states and introduction to the generic idea

2.1. Characterization of Gaussian states

Let us first establish what we mean by general Gaussian states [2, 30–33]. Consider for this N bosonic modes with annihilation operators that we collect into the vector $\hat{\mathbf{a}} = (\hat{a}_1, \hat{a}_2, \dots, \hat{a}_N)^T$, satisfying canonical commutation relations $[\hat{a}_j, \hat{a}_j^\dagger] = \delta_{jl}$ and $[\hat{a}_j, \hat{a}_l] = 0$. We introduce a notation in which the transpose symbol transposes vector arrays but without affecting the operators that make them up, so that $\hat{\mathbf{a}}$ is a column vector while $\hat{\mathbf{a}}^T = (\hat{a}_1, \hat{a}_2, \dots, \hat{a}_N)$ is a row vector. In contrast, the dagger symbol will affect both the vector arrays and the internal operators, so that $\hat{\mathbf{a}}^\dagger = (\hat{a}_1^\dagger, \hat{a}_2^\dagger, \dots, \hat{a}_N^\dagger)$ is a row vector with creation operators as entries, with corresponding column vector $\hat{\mathbf{a}}^{\dagger T}$. These symbols act as usual on any complex matrix \mathcal{M} , that is, $(\mathcal{M}^T)_{jl} = \mathcal{M}_{lj}$ and $(\mathcal{M}^\dagger)_{jl} = \mathcal{M}_{lj}^*$.

Any Gaussian state (up to a trivial displacement) can be generated by applying a Gaussian unitary \hat{G} to a thermal state of all modes [2, 30–33]

$$\hat{\rho}_G(\bar{\mathbf{n}}) = \hat{G} \hat{\rho}_{\text{th}}(\bar{\mathbf{n}}) \hat{G}^\dagger. \quad (1)$$

with $\hat{\rho}_{\text{th}}(\bar{\mathbf{n}}) = \otimes_{j=1}^N \hat{\rho}_{\text{th},j}(\bar{n}_j)$, where $\bar{\mathbf{n}} = (\bar{n}_1, \dots, \bar{n}_N)$ collects the number of thermal excitations of the modes, which in turn fix the entropy or mixedness of the state of the system, and

$$\hat{\rho}_{\text{th},j}(\bar{n}_j) = \frac{e^{-\kappa_j \hat{a}_j^\dagger \hat{a}_j}}{\text{tr} \left\{ e^{-\kappa_j \hat{a}_j^\dagger \hat{a}_j} \right\}}, \quad (2)$$

is a thermal state for a mode with normalized inverse temperature κ_j , related to the number of excitations by the Bose–Einstein distribution $\bar{n}_j = (e^{\kappa_j} - 1)^{-1}$. The Gaussian unitary does not add any extra entropy to the state, but changes the correlations (including entanglement) between the modes. Such unitaries are characterized by effecting a so-called Bogoliubov transformation, which mixes linearly annihilation and creation operators as

$$\hat{G}^\dagger \hat{\mathbf{a}} \hat{G} = \mathcal{A} \hat{\mathbf{a}} + \mathcal{B} \hat{\mathbf{a}}^{\dagger T} \equiv \hat{\mathbf{A}}, \quad (3)$$

with $N \times N$ complex matrices \mathcal{A} and \mathcal{B} subject to the constraints

$$\mathcal{A} \mathcal{B}^T = \mathcal{B} \mathcal{A}^T, \quad \mathcal{A} \mathcal{A}^\dagger = \mathcal{B} \mathcal{B}^\dagger + \mathcal{I}, \quad (4)$$

where \mathcal{I} is the $N \times N$ identity, such that the transformed annihilation operators $\hat{\mathbf{A}}$ satisfy canonical commutation relations just like the original ones.

Pure states, for which $\bar{\mathbf{n}} = 0$, correspond to the Gaussian unitary acting on the vacuum of the original modes,

$$|G\rangle = \hat{G} |\text{vac}\rangle_a, \quad \text{where } \hat{\mathbf{a}} |\text{vac}\rangle_a = 0. \quad (5)$$

In turn, this state is nothing but the vacuum of the transformed modes, that is, $|G\rangle = |\text{vac}\rangle_A$, where $\hat{\mathbf{A}} |\text{vac}\rangle_A = 0$.

Our protocol for the dissipative generation of Gaussian states is most naturally formulated in terms of the matrices \mathcal{A} and \mathcal{B} . However, Gaussian states are most commonly characterized via the covariance matrix, which identifies its Wigner function in phase space [2, 30–33]. It is then useful to know the relation between

these two descriptions. Defining the vector of quadratures $\hat{\mathbf{r}} = (\hat{x}_1, \dots, \hat{x}_N, \hat{p}_1, \dots, \hat{p}_N)^T$, with $\hat{x}_j = \hat{a}_j + \hat{a}_j^\dagger$ and $\hat{p}_j = -i(\hat{a}_j - \hat{a}_j^\dagger)$, the covariance matrix elements are defined as $V_{mn} = \langle \hat{r}_m \hat{r}_n + \hat{r}_n \hat{r}_m \rangle / 2$. Using the commutation relations $[\hat{r}_m, \hat{r}_n] = 2i\mathcal{W}_{mn}$ and the relation $\hat{\mathbf{r}} = \mathcal{T}\hat{\boldsymbol{\alpha}}$, with

$$\hat{\boldsymbol{\alpha}} = \begin{pmatrix} \hat{\mathbf{a}} \\ \hat{\mathbf{a}}^{\dagger T} \end{pmatrix} = (\hat{a}_1, \dots, \hat{a}_N, \hat{a}_1^\dagger, \dots, \hat{a}_N^\dagger)^T, \quad (6a)$$

$$\mathcal{T} = \begin{pmatrix} \mathcal{I} & \mathcal{I} \\ -i\mathcal{I} & i\mathcal{I} \end{pmatrix}, \quad (6b)$$

$$\mathcal{W} = \begin{pmatrix} 0 & \mathcal{I} \\ -\mathcal{I} & 0 \end{pmatrix}, \quad (6c)$$

the covariance matrix can be written as

$$V = \mathcal{T} \underbrace{\langle \hat{\boldsymbol{\alpha}} \hat{\boldsymbol{\alpha}}^T \rangle}_{C} \mathcal{T}^T - i\mathcal{W}. \quad (7)$$

In turn, the complex covariance matrix C can be easily found in terms of \mathcal{A} and \mathcal{B} as

$$\begin{aligned} C &= \text{tr} \left\{ \hat{\rho}_G(\bar{\mathbf{n}}) \hat{\boldsymbol{\alpha}} \hat{\boldsymbol{\alpha}}^T \right\} = \text{tr} \left\{ \hat{\rho}_{\text{th}}(\bar{\mathbf{n}}) \hat{G}^\dagger \hat{\boldsymbol{\alpha}} \hat{\boldsymbol{\alpha}}^T \hat{G} \right\} \\ &= \begin{pmatrix} \mathcal{J}(\mathcal{A}, \mathcal{B}, \mathcal{B}, \mathcal{A}) & \mathcal{J}(\mathcal{A}, \mathcal{A}^*, \mathcal{B}, \mathcal{B}^*) \\ \mathcal{J}(\mathcal{B}^*, \mathcal{B}, \mathcal{A}^*, \mathcal{A}) & \mathcal{J}(\mathcal{B}^*, \mathcal{A}^*, \mathcal{A}^*, \mathcal{B}^*) \end{pmatrix}, \end{aligned} \quad (8)$$

where $\mathcal{J}(\mathcal{X}, \mathcal{Y}, \mathcal{Z}, \mathcal{R}) = \mathcal{X}(\mathcal{I} + \bar{\mathcal{N}})\mathcal{Y}^T + \mathcal{Z}\bar{\mathcal{N}}\mathcal{R}^T$, $\bar{\mathcal{N}} = \text{diag}(\bar{\mathbf{n}})$ is a diagonal matrix containing all the thermal populations in the diagonal, and we have used (3) in the form

$$\hat{G}^\dagger \hat{\boldsymbol{\alpha}} \hat{G} = \begin{pmatrix} \mathcal{A}\hat{\mathbf{a}} + \mathcal{B}\hat{\mathbf{a}}^{\dagger T} \\ \mathcal{A}^*\hat{\mathbf{a}}^{\dagger T} + \mathcal{B}^*\hat{\mathbf{a}} \end{pmatrix}, \quad (9)$$

as well as $\text{tr} \left\{ \hat{\rho}_{\text{th}}(\bar{\mathbf{n}}) \hat{\mathbf{a}}^{\dagger T} \hat{\mathbf{a}}^T \right\} = \bar{\mathcal{N}}$, $\text{tr} \left\{ \hat{\rho}_{\text{th}}(\bar{\mathbf{n}}) \hat{\mathbf{a}} \hat{\mathbf{a}}^\dagger \right\} = \mathcal{I} + \bar{\mathcal{N}}$, and $\text{tr} \left\{ \hat{\rho}_{\text{th}}(\bar{\mathbf{n}}) \hat{\mathbf{a}} \hat{\mathbf{a}}^T \right\} = 0 = \text{tr} \left\{ \hat{\rho}_{\text{th}}(\bar{\mathbf{n}}) \hat{\mathbf{a}}^{\dagger T} \hat{\mathbf{a}}^\dagger \right\}$. These expressions are highly simplified in the case of pure states, for which $\bar{\mathcal{N}} = 0$. In such case, (6)–(8) lead to

$$V = 2 \begin{pmatrix} \text{Re}\{\mathcal{D}_+\} - \mathcal{I}/2 & -\text{Im}\{\mathcal{D}_-\} \\ \text{Im}\{\mathcal{D}_+\} & \text{Re}\{\mathcal{D}_-\} - \mathcal{I}/2 \end{pmatrix}, \quad (10)$$

where $\mathcal{D}_\pm = \mathcal{A}\mathcal{A}^\dagger \pm \mathcal{A}\mathcal{B}^T$. This expression connects the Hilbert space description of Gaussian states in terms of Gaussian unitaries acting on thermal states (that is, in terms of $\bar{\mathbf{n}}$, \mathcal{A} , and \mathcal{B}) with the phase-space description in terms of the covariance matrix V . An explicit example of how to use this connection is given in section 5 when considering GHZ states.

In the following, and as we did in this section, indices j , l , and k will run from 1 to N , while index m will run up to $2N$.

2.2. Basic idea for the dissipative generation of Gaussian states

Our strategy in order to generate the multimode Gaussian states introduced above is similar to the one we introduced in previous works for single-mode and two-mode squeezed states [28, 29]. As summarized in figure 1, we couple N modes of linear superconducting circuits with distinct frequencies $\{\omega_j\}_{j=1,2,\dots,N}$ to N superconducting qubits also with distinct frequencies $\{\varepsilon_j\}_{j=1,2,\dots,N}$, as described by the Hamiltonian (in section 7 we explain how to avoid all-to-all couplings, and implement the idea with local couplings only)

$$\hat{H}(t) = \sum_{j=1}^N \left(\omega_j \hat{n}_j + \frac{\varepsilon_j}{2} \hat{\sigma}_j^z \right) + \sum_{j,l=1}^N g_{jl} (\hat{\sigma}_j + \hat{\sigma}_j^\dagger) (\hat{a}_l + \hat{a}_l^\dagger) + \sum_{j=1}^N \left[\sum_{m=1}^{2N} \Omega_{jm} \eta_{jm} \cos(\Omega_{jm} t + \phi_{jm}) \right] \hat{\sigma}_j^z, \quad (11)$$

with number operators $\hat{n}_j = \hat{a}_j^\dagger \hat{a}_j$, and Pauli operators $\hat{\sigma}_j^z = |e\rangle_j \langle e| - |g\rangle_j \langle g|$ and $\hat{\sigma}_j = |g\rangle_j \langle e|$ for qubit j with ground and excited states $|g\rangle_j$ and $|e\rangle_j$, respectively. Note that we are using \hbar units for the Hamiltonian, so that all parameters have frequency units for convenience. We also take all the parameters real and positive for definiteness. We assume that all direct processes are far off resonant, $|\varepsilon_j \pm \omega_l| \gg g_{jl}$, and add a temporal modulation of the qubit frequencies that will help the system bring certain processes to resonance effectively. In particular, in general we will need to modulate each qubit with $2N$ different frequencies Ω_{jm} , with

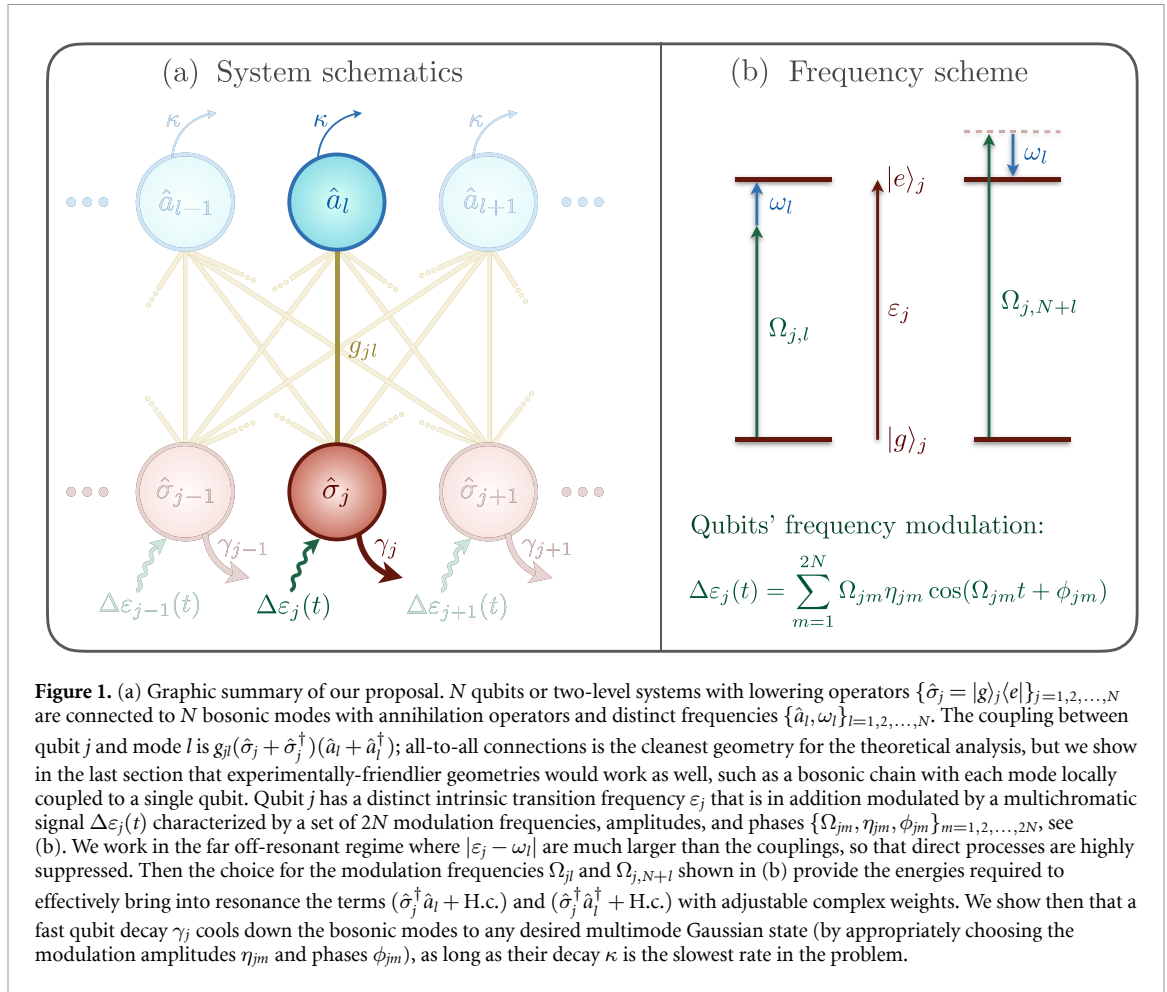


Figure 1. (a) Graphic summary of our proposal. N qubits or two-level systems with lowering operators $\{\hat{\sigma}_j = |g\rangle_j\langle e|\}_{j=1,2,\dots,N}$ are connected to N bosonic modes with annihilation operators and distinct frequencies $\{\hat{a}_l, \omega_l\}_{l=1,2,\dots,N}$. The coupling between qubit j and mode l is $g_{jl}(\hat{\sigma}_j + \hat{\sigma}_j^\dagger)(\hat{a}_l + \hat{a}_l^\dagger)$; all-to-all connections is the cleanest geometry for the theoretical analysis, but we show in the last section that experimentally-friendlier geometries would work as well, such as a bosonic chain with each mode locally coupled to a single qubit. Qubit j has a distinct intrinsic transition frequency ε_j that is in addition modulated by a multichromatic signal $\Delta\varepsilon_j(t)$ characterized by a set of $2N$ modulation frequencies, amplitudes, and phases $\{\Omega_{jm}, \eta_{jm}, \phi_{jm}\}_{m=1,2,\dots,2N}$, see (b). We work in the far off-resonant regime where $|\varepsilon_j - \omega_l|$ are much larger than the couplings, so that direct processes are highly suppressed. Then the choice for the modulation frequencies $\Omega_{j,l}$ and $\Omega_{j,N+l}$ shown in (b) provide the energies required to effectively bring into resonance the terms $(\hat{\sigma}_j^\dagger \hat{a}_l + \text{H.c.})$ and $(\hat{\sigma}_j \hat{a}_l^\dagger + \text{H.c.})$ with adjustable complex weights. We show then that a fast qubit decay γ_j cools down the bosonic modes to any desired multimode Gaussian state (by appropriately choosing the modulation amplitudes η_{jm} and phases ϕ_{jm}), as long as their decay κ is the slowest rate in the problem.

corresponding (normalized) amplitudes $\eta_{jm} \ll 1$ and phases ϕ_{jm} , in order to be able to tune all the possible couplings between the modes and the qubits. Of course, for specific states the final count might be smaller.

As we rigorously show in the next section, choosing the modulation frequencies (see figure 1)

$$\Omega_{jl} = \varepsilon_j - \omega_l, \quad \Omega_{j,N+l} = \varepsilon_j + \omega_l, \quad j, l = 1, 2, \dots, N \tag{12}$$

we will be able to control all couplings of the qubits' ladder operators to the modes' annihilation and creation operators, generating the effective Hamiltonian

$$\hat{H}_{\text{eff}} = - \sum_{j=1}^N \bar{g}_j \hat{A}_j \hat{\sigma}_j^\dagger + \text{H.c.}, \tag{13}$$

where \bar{g}_j are some effective couplings and \hat{A}_j are the transformed annihilation operators (3) corresponding to the Gaussian state $|G\rangle$ that we want to generate. Let us remark that Ω_{jl} is precisely the energy missing to bring the term $\hat{\sigma}_j \hat{a}_l^\dagger$ (and its Hermitian conjugate) to resonance, see figure 1(b); similarly $\Omega_{j,N+l}$ provides the energy missing for the $\hat{\sigma}_j \hat{a}_l$ process to play a role, see figure 1(b). It is then intuitive that, in the right picture and under the right conditions, (13) will capture the physics of the dynamics generated by (11). We will prove this rigorously shortly.

The final step consists on introducing a strong radiative decay on each qubit at rate $\gamma_j \gg |\bar{g}_j|$. Hence, every time an excitation is transferred from modes \hat{A} to the qubits via (13), the excitation will be quickly lost before it can come back to the photonic modes, which will then be cooled down to their vacuum state $|vac\rangle_A$ at rate $|\bar{g}_j|^2/\gamma_j$ [28, 29]. In particular, eliminating adiabatically the qubits using standard techniques [28, 29, 33], the reduced state $\hat{\rho}$ of the bosonic modes is easily shown to obey the following master equation:

$$\frac{d\hat{\rho}}{dt} = \sum_{j=1}^N \left(\frac{|\bar{g}_j|^2}{\gamma_j} \mathcal{D}_{A_j}[\hat{\rho}] + \kappa \mathcal{D}_{a_j}[\hat{\rho}] \right), \tag{14}$$

with $\mathcal{D}_C[\hat{\rho}] = 2\hat{C}\hat{\rho}\hat{C}^\dagger - \hat{C}^\dagger\hat{C}\hat{\rho} - \hat{\rho}\hat{C}^\dagger\hat{C}$. Here we have taken into account the decay of the original modes \hat{a}_j at rates κ (taken all equal for simplicity). In the limit of large cooperativities $|\bar{g}_j|^2/\gamma_j\kappa \gg 1$ the local decays \mathcal{D}_{a_j} are negligible, so that the dominant \mathcal{D}_{A_j} terms will steer the state into the vacuum of the \hat{A}_j modes, that is, the state $|G\rangle$ of equation (5) we were seeking. If the cooperativities are not large enough, the local decays will introduce some entropy in the final state, so by tailoring them we can even control the type of mixed Gaussian state $\hat{\rho}_G(\bar{n})$ that we want to generate.

In the following we elaborate on these ideas and consider specific examples.

3. Effective Hamiltonian and limitations

We now rigorously show how to obtain the effective Hamiltonian (13) from the time-dependent Hamiltonian (11). We first need to move to the interaction picture defined by the transformation operator

$$\hat{U}(t) = \exp\left(-i \int_0^t dt' \hat{H}_0(t')\right), \text{ with } \hat{H}_0 = \sum_{j=1}^N \left\{ \omega_j \hat{n}_j + \left[\frac{\varepsilon_j}{2} + \sum_{m=1}^{2N} \Omega_{jm} \eta_{jm} \cos(\Omega_{jm}t + \phi_{jm}) \right] \hat{\sigma}_j^z \right\}, \quad (15)$$

where states evolve according to the transformed Hamiltonian [33] $\tilde{H}(t) = \hat{U}^\dagger(t)\hat{H}(t)\hat{U}(t) - \hat{H}_0(t)$. Next we apply the Baker–Campbell–Hausdorff formula [33] to write

$$\hat{U}^\dagger(t)\hat{a}_j\hat{U}(t) = e^{-i\omega_j t}\hat{a}_j, \quad (16a)$$

$$\hat{U}^\dagger(t)\hat{\sigma}_j\hat{U}(t) = e^{-i[\varepsilon_j + \sum_{m=1}^{2N} 2\eta_{jm} \sin(\Omega_{jm}t + \phi_{jm})]t}\hat{\sigma}_j, \quad (16b)$$

and use the fact that the sine function is the generator of Bessel functions, so

$$e^{2i\eta \sin(\Omega t + \phi)} = \sum_{n=-\infty}^{+\infty} J_n(2\eta) e^{in(\Omega t + \phi)}, \quad (17)$$

where $J_{n>0}(2\eta) \xrightarrow{\eta \ll \sqrt{n+1}} \eta^n/n!$ are the Bessel functions, which satisfy $J_{-n}(2\eta) = (-1)^n J_n(2\eta)$. The transformed Hamiltonian takes then the form

$$\tilde{H}(t) = \sum_{jl=1}^N g_{jl} \hat{\sigma}_j^\dagger \left[\alpha_{jl}(t) \hat{a}_l + \beta_{jl}(t) \hat{a}_l^\dagger \right] + \text{H.c.}, \quad (18)$$

with

$$\alpha_{jl}(t) = \sum_{n_1 n_2 \dots n_{2N} = -\infty}^{+\infty} J_{n_1}(2\eta_{j1}) J_{n_2}(2\eta_{j2}) \dots J_{n_{2N}}(2\eta_{j,2N}) e^{-i(\omega_l - \varepsilon_j - \sum_{m=1}^{2N} n_m \Omega_{jm})t} e^{i \sum_{m=1}^{2N} n_m \phi_{jm}}, \quad (19a)$$

$$\beta_{jl}(t) = \sum_{n_1 n_2 \dots n_{2N} = -\infty}^{+\infty} J_{n_1}(2\eta_{j1}) J_{n_2}(2\eta_{j2}) \dots J_{n_{2N}}(2\eta_{j,2N}) e^{i(\omega_l + \varepsilon_j + \sum_{m=1}^{2N} n_m \Omega_{jm})t} e^{i \sum_{m=1}^{2N} n_m \phi_{jm}}. \quad (19b)$$

These time-dependent couplings are a sum of terms oscillating at different frequencies, but we next prove that a judicious choice of modulation amplitudes η_{jm} , phases ϕ_{jm} , and frequencies Ω_{jm} will make the contribution from most terms vanish effectively, except for some static ones that we will use to match the form (13) of the effective Hamiltonian that we seek. Let us in particular choose the modulation frequencies Ω_{jm} as we explained in the previous section, equation (12). Then, we define the frequencies of the different terms in (19) as

$$\nu_{jl;\mathbf{n}}^{(\alpha)} = \omega_l - \varepsilon_j - \sum_{m=1}^{2N} n_m \Omega_{jm} = \omega_l(1 + n_l - n_{N+l}) - \varepsilon_j \left(1 + \sum_{m=1}^{2N} n_m \right) + \sum_{l \neq k=1}^N \omega_k (n_k - n_{N+k}), \quad (20a)$$

$$\nu_{jl;\mathbf{n}}^{(\beta)} = \omega_l + \varepsilon_j + \sum_{m=1}^{2N} n_m \Omega_{jm} = \omega_l(1 - n_l + n_{N+l}) + \varepsilon_j \left(1 + \sum_{m=1}^{2N} n_m \right) - \sum_{l \neq k=1}^N \omega_k (n_k - n_{N+k}), \quad (20b)$$

where we have introduced a vector $\mathbf{n} = (n_1, n_2, \dots, n_{2N})$ containing the Bessel indices. Let us also define a quantity that we will call the η -order, $|n| = \sum_{m=1}^{2N} |n_m|$, which for each term $J_{n_1}(2\eta_{j1}) J_{n_2}(2\eta_{j2}) \dots J_{n_{2N}}(2\eta_{j,2N})$ provides the order of the polynomial approximation in the small modulation amplitudes η_{jm} . We will say

that an index combination \mathbf{n} is resonant when $\nu_{j\mathbf{l};\mathbf{n}}^{(\chi)} = 0$, where χ can be either α or β . For each $\alpha_{j\mathbf{l}}$ and $\beta_{j\mathbf{l}}$ we already have a resonant term at η -order $|\mathbf{n}| = 1$, since

$$\nu_{j\mathbf{l};n_1=0,\dots,n_{l-1}=0,n_l=-1,n_{l+1}=0,\dots,n_{2N}=0}^{(\alpha)} = 0, \quad (21a)$$

$$\nu_{j\mathbf{l};n_1=0,\dots,n_{N+l-1}=0,n_{N+l}=-1,n_{N+l+1}=0,\dots,n_{2N}=0}^{(\beta)} = 0. \quad (21b)$$

Ideally, we would like any other resonances to appear only at large η -order $|\mathbf{n}|$, so that their corresponding contribution to the coupling is highly suppressed as $\eta^{|\mathbf{n}|}$. Lower η -order frequencies, on the other hand, should satisfy $|\nu_{j\mathbf{l};\mathbf{n}}^{(\chi)}| \gg |g_{j\mathbf{l}}J_{n_1}(2\eta_{j1})J_{n_2}(2\eta_{j2})\dots J_{n_{2N}}(2\eta_{j,2N})|$, so that their contribution can be neglected by virtue of the rotating-wave approximation. While it is not difficult to check that there are no resonances at η -order $|\mathbf{n}| = 2$ (for example, by doing an exhaustive check of all available combinations of Bessel indices with any symbolic math software), we already find unavoidable resonances at η -order $|\mathbf{n}| = 3$, which we discuss in detail at the end of this section. For the sake of argumentation, let us however proceed for now assuming that all contributions are negligible in (21) except the $|\mathbf{n}| = 1$ ones, and how this allows us to obtain the effective Hamiltonian (13). Under such assumption, the effective couplings can be rewritten as

$$\alpha_{j\mathbf{l}} \approx J_0(2\eta_{j1})\dots J_0(2\eta_{j,l-1})J_{-1}(2\eta_{jl})J_0(2\eta_{j,l+1})\dots J_0(2\eta_{j,2N})e^{-i\phi_{j\mathbf{l}}} \approx -\eta_{j\mathbf{l}}e^{-i\phi_{j\mathbf{l}}}, \quad (22a)$$

$$\beta_{j\mathbf{l}} \approx J_0(2\eta_{j1})\dots J_0(2\eta_{j,N+l-1})J_{-1}(2\eta_{j,N+l})J_0(2\eta_{j,N+l+1})\dots J_0(2\eta_{j,2N})e^{-i\phi_{j,N+l}} \approx -\eta_{j,N+l}e^{-i\phi_{j,N+l}}, \quad (22b)$$

where we have assumed that the modulation amplitudes $\eta_{j\mathbf{l}}$ are small enough such that the lowest-order approximation of the Bessel functions hold, in particular $J_0(2\eta) \approx 1$ and $J_{-1}(2\eta) \approx -\eta$. The interaction-picture Hamiltonian (18) turns then into an effective Hamiltonian

$$\tilde{H}_{\text{eff}} = -\sum_{j=1}^N \left[\sum_{l=1}^N g_{j\mathbf{l}} \left(\eta_{j\mathbf{l}} e^{-i\phi_{j\mathbf{l}}} \hat{a}_l + \eta_{j,N+l} e^{-i\phi_{j,N+l}} \hat{a}_l^\dagger \right) \right] \hat{\sigma}_j^\dagger + \text{H.c.}, \quad (23)$$

which has exactly the form in (13), making the correspondence

$$\bar{g}_j \hat{A}_j = \sum_{l=1}^N g_{j\mathbf{l}} \left(\eta_{j\mathbf{l}} e^{-i\phi_{j\mathbf{l}}} \hat{a}_l + \eta_{j,N+l} e^{-i\phi_{j,N+l}} \hat{a}_l^\dagger \right) \quad (24a)$$

$$\downarrow \\ \bar{g}_j \mathcal{A}_{j\mathbf{l}} = g_{j\mathbf{l}} \eta_{j\mathbf{l}} e^{-i\phi_{j\mathbf{l}}}, \quad \bar{g}_j \mathcal{B}_{j\mathbf{l}} = g_{j\mathbf{l}} \eta_{j,N+l} e^{-i\phi_{j,N+l}}, \quad j, l = 1, 2, \dots, N. \quad (24b)$$

Now, since the modulation amplitudes $\eta_{j\mathbf{m}}$ and phases $\phi_{j\mathbf{m}}$ can be freely chosen (just with the requirement that the amplitudes must be small), this expression seems to suggest that we indeed can access any multimode Gaussian state we want, just with the subtlety that the effective couplings $|\bar{g}_j|$ could become too small, leading to slow cooling rates $|\bar{g}_j|^2/\gamma_j$. Equation (24b) fixes the modulation phases as

$$\phi_{j\mathbf{l}} = -\arg\{\mathcal{A}_{j\mathbf{l}}\}, \quad \phi_{j,N+l} = -\arg\{\mathcal{B}_{j\mathbf{l}}\}, \quad (25)$$

and considering for simplicity the case of homogeneous coupling, $g_{j\mathbf{l}} = g \forall j\mathbf{l}$, the modulation amplitudes need to satisfy

$$\eta_{j\mathbf{l}} = \frac{\bar{g}_j}{g} |\mathcal{A}_{j\mathbf{l}}|, \quad \eta_{j,N+l} = \frac{\bar{g}_j}{g} |\mathcal{B}_{j\mathbf{l}}|. \quad (26)$$

Since the effective couplings are still to be determined, this expressions do not fix all modulation amplitudes, in particular allowing us to fix N of them (one for each value of j) at will. Let us denote by \bar{l}_j the value of l that we pick as reference for each j , so that $\{\eta_{j\bar{l}_j}\}_{j=1,2,\dots,N}$ are the amplitudes that we fix to whatever value we want. Assuming then that $\mathcal{A}_{j\bar{l}_j} \neq 0$ (otherwise, we just use a different reference l value), this fixes the rest of amplitudes as

$$\eta_{j\mathbf{l}} = \frac{|\mathcal{A}_{j\mathbf{l}}|}{|\mathcal{A}_{j\bar{l}_j}|} \eta_{j\bar{l}_j}, \quad \eta_{j,N+l} = \frac{|\mathcal{B}_{j\mathbf{l}}|}{|\mathcal{A}_{j\bar{l}_j}|} \eta_{j\bar{l}_j}. \quad (27)$$

The ratios $|\mathcal{A}_{jl}/\mathcal{A}_{\bar{j}\bar{l}}|$ and $|\mathcal{B}_{jl}/\mathcal{A}_{\bar{j}\bar{l}}|$ can be larger than one, so one needs to be careful to choose the reference amplitudes $\eta_{\bar{j}\bar{l}}$ so as to keep the rest of the amplitudes η_{jm} small. Inserting these expressions back in (26), we obtain the effective couplings

$$\bar{g}_j = \frac{\eta_{\bar{j}\bar{l}}}{|\mathcal{A}_{\bar{j}\bar{l}}|} g. \quad (28)$$

Before moving on to examples, we need to comment about the limitations imposed by the resonance at η -order $|n| = 3$. In particular, for a given frequency $\nu_{jl;n}^{(\chi)}$ it is always possible to find $N - 1$ resonances with $|n| = 3$ that make it vanish exactly: we can make each of the three terms adding up in the final forms of (20a) and (20b) vanish independently by choosing $(n_l, n_{N+l}) = (0, 1)$ for $\nu_{jl;n}^{(\alpha)}$ and $(n_l, n_{N+l}) = (1, 0)$ for $\nu_{jl;n}^{(\beta)}$, and then $n_k = n_{N+k} = -1$ for any other $k \neq l$. Hence, a more precise expression for the couplings α_{jl} and β_{jl} up to third order in the modulation amplitudes η_{jl} would be

$$\alpha_{jl} \approx -\eta_{jl} e^{-i\phi_{jl}} \left[1 - \sum_{m=1}^{2N} \left(1 - \frac{\delta_{ml}}{2} \right) \eta_{jm}^2 \right] + \sum_{l \neq k=1}^N \eta_{j,N+l} \eta_{jk} \eta_{j,N+k} e^{i(\phi_{j,N+l} - \phi_{jk} - \phi_{j,N+k})}, \quad (29a)$$

$$\beta_{jl} \approx -\eta_{j,N+l} e^{-i\phi_{j,N+l}} \left[1 - \sum_{m=1}^{2N} \left(1 - \frac{\delta_{m,N+l}}{2} \right) \eta_{jm}^2 \right] + \sum_{l \neq k=1}^N \eta_{j,l} \eta_{jk} \eta_{j,N+k} e^{i(\phi_{j,l} - \phi_{jk} - \phi_{j,N+k})}. \quad (29b)$$

Note that we have also included the third order correction in η_{jl} that comes from (22) when expanding the Bessel functions as $J_0(2\eta) = 1 - \eta^2$ and $J_{-1}(2\eta) \approx -\eta + \eta^3/2$. Assuming that all the amplitudes are of the same order η , we then see that by neglecting these contributions, we are making a relative mistake of order $N\eta^2$ in the worst case. Depending on the accuracy with which we want to generate the Gaussian state, this might need to be considered carefully. Of course, one can always include this contribution when doing the matching (24b) and choose the amplitudes and phases accordingly, but then the construction becomes more cumbersome. We will come back to this issue in section 6 with examples that will allow us to show that even for large N and large entanglement levels these third-order corrections do not impose serious constraints to our proposal.

4. Example 1: continuous-variable cluster states

4.1. Cluster states

As a specific example, we consider in this section the generation of the class of so-called continuous-variable cluster states [4, 34, 35]. These are the states explicitly used in measurement-based quantum computation [4]. They rely on the application of the continuous-variable analog of the controlled- Z gate, which for two modes with indices j and l is defined as $\exp(iq\hat{x}_j\hat{x}_l/4)$, where we call $q \in \mathbb{R}$ the control- Z parameter. In loose terms, the gate applies a momentum translation on mode j that depends on the position of mode l (and vice versa). Cluster states of N modes are then defined through the application of controlled- Z gates to a zero-momentum eigenstate of all modes [4, 34, 35]. In particular, consider an $N \times N$ real symmetric matrix \mathcal{Q} whose elements are the control- Z parameters for each pair of modes, which defines the controlled- Z gate for the bosonic modes

$$\hat{C}_Z(\mathcal{Q}) = e^{\frac{i}{4}\hat{\mathbf{x}}^T \mathcal{Q} \hat{\mathbf{x}}} = e^{\frac{i}{4} \sum_{j,l=1}^N \mathcal{Q}_{jl} \hat{x}_j \hat{x}_l}. \quad (30)$$

We gather the positions and momenta in the vectors $\hat{\mathbf{x}} = (\hat{x}_1, \dots, \hat{x}_N)^T$ and $\hat{\mathbf{p}} = (\hat{p}_1, \dots, \hat{p}_N)^T$. Applying this Gaussian unitary (30) to momentum eigenstates leads to an unnormalizable state. In order to define physical cluster states, one then considers momentum-squeezed states instead, obtained by applying the squeezing operators $\hat{S}_j(r) = \exp[r(\hat{a}_j^{\dagger 2} - \hat{a}_j^2)/2]$ to the vacuum state. The resulting states converge to ideal cluster states in the $r \rightarrow \infty$ limit and have the form

$$|\psi(\mathcal{Q}, r)\rangle = \underbrace{\hat{C}_Z(\mathcal{Q}) \hat{S}_N(r) \dots \hat{S}_2(r) \hat{S}_1(r)}_{\hat{G}} |\text{vac}\rangle_a. \quad (31)$$

These states are already written as the action of a Gaussian unitary \hat{G} on the vacuum of the original modes as in (5). Noting that

$$\hat{C}_Z^\dagger(\mathcal{Q})\hat{\mathbf{x}}\hat{C}_Z(\mathcal{Q}) = \hat{\mathbf{x}}, \quad (32a)$$

$$\hat{C}_Z^\dagger(\mathcal{Q})\hat{\mathbf{p}}\hat{C}_Z(\mathcal{Q}) = \hat{\mathbf{p}} + \mathcal{Q}\hat{\mathbf{x}}, \quad (32b)$$

$$\hat{S}_j^\dagger(r)\hat{a}_j\hat{S}_j(r) = \hat{a}_j \cosh r + \hat{a}_j^\dagger \sinh r, \quad (32c)$$

$$\hat{S}_j^\dagger(r)\hat{x}_j\hat{S}_j(r) = e^r \hat{x}_j, \quad (32d)$$

$$\hat{S}_j^\dagger(r)\hat{p}_j\hat{S}_j(r) = e^{-r} \hat{p}_j, \quad (32e)$$

as easily found by applying the Baker–Campbell–Hausdorff formula [33], it is then easy to see that the variances of the quadratures $\hat{\mathbf{X}} = \hat{\mathbf{x}}$ and $\hat{\mathbf{P}} = \hat{\mathbf{p}} - \mathcal{Q}\hat{\mathbf{x}}$ (which form a conjugate set, since they obey canonical commutation relations) satisfy

$$\text{var}(\hat{X}_j) = e^{2r} \quad \text{and} \quad \text{var}(\hat{P}_j) = e^{-2r}, \quad \forall j, \quad (33)$$

where $\text{var}(\hat{B}) = \langle \hat{B}^2 \rangle - \langle \hat{B} \rangle^2$. Hence, in a cluster state, one finds correlations between the momenta \hat{p}_j and the combinations $(\mathcal{Q}\hat{\mathbf{x}})_j$ of position operators. These correlations are beyond what's achievable for a coherent state (corresponding to $r = 0$) or mixtures of coherent states (lower bounded by unit quadrature variances), all these known as classical states, since they lead to a positive and normalizable Glauber–Sudarshan distribution [36]; in other words, states satisfying (33) are non-classical according to this notion of non-classicality.

4.2. Generating cluster states with our scheme

Let us now particularize to these cluster states the choice of modulation amplitudes η_{jm} and phases ϕ_{jm} that we did in (27) for general Gaussian states, and discuss what we get. First we need to find the matrices \mathcal{A} and \mathcal{B} defined for a general Gaussian unitary in (3), but particularized to the one associated with the cluster states (31). Using (32) and the relation $\hat{\mathbf{a}} = (\hat{\mathbf{x}} + i\hat{\mathbf{p}})/2$ between quadratures and annihilation and creation operators, we get

$$\hat{G}^\dagger \hat{\mathbf{a}} \hat{G} = \frac{1}{2} \hat{C}_Z^\dagger(\mathcal{Q}) (e^r \hat{\mathbf{x}} + ie^{-r} \hat{\mathbf{p}}) \hat{C}_Z(\mathcal{Q}) = \frac{1}{2} (e^r \mathcal{I} + ie^{-r} \mathcal{Q}) \hat{\mathbf{x}} + \frac{i}{2} e^{-r} \hat{\mathbf{p}}. \quad (34)$$

In turn, using $\hat{\mathbf{x}} = \hat{\mathbf{a}} + \hat{\mathbf{a}}^{\dagger T}$ and $i\hat{\mathbf{p}} = \hat{\mathbf{a}} - \hat{\mathbf{a}}^{\dagger T}$, we then obtain

$$\hat{G}^\dagger \hat{\mathbf{a}} \hat{G} = \left(\mathcal{I} \cosh r + \frac{i}{2} e^{-r} \mathcal{Q} \right) \hat{\mathbf{a}} + \left(\mathcal{I} \sinh r + \frac{i}{2} e^{-r} \mathcal{Q} \right) \hat{\mathbf{a}}^{\dagger T}, \quad (35)$$

leading to

$$\mathcal{A} = \mathcal{I} \cosh r + ie^{-r} \mathcal{Q}/2, \quad (36a)$$

$$\mathcal{B} = \mathcal{I} \sinh r + ie^{-r} \mathcal{Q}/2. \quad (36b)$$

Using now relations (25) and (27), and choosing in this case $\bar{l}_j = j$, that is, we take η_{jj} as the reference amplitudes (since \mathcal{A}_{jj} is different than zero for all cluster states), we then obtain

$$\eta_{jl} = \eta_{jj} \sqrt{\frac{4\delta_{jl} \cosh^2 r + e^{-2r} \mathcal{Q}_{jl}^2}{4 \cosh^2 r + e^{-2r} \mathcal{Q}_{jj}^2}}, \quad (37a)$$

$$\eta_{j,N+l} = \eta_{jj} \sqrt{\frac{4\delta_{jl} \sinh^2 r + e^{-2r} \mathcal{Q}_{jl}^2}{4 \cosh^2 r + e^{-2r} \mathcal{Q}_{jj}^2}}, \quad (37b)$$

$$\phi_{jl} = \begin{cases} -\arg\{2 \cosh r + ie^{-r} \mathcal{Q}_{jj}\}, & l = j \\ -\text{sign}\{\mathcal{Q}_{jl}\} \times \pi/2 & l \neq j \end{cases}, \quad (37c)$$

$$\phi_{j,N+l} = \begin{cases} -\arg\{2 \sinh r + ie^{-r} \mathcal{Q}_{jj}\}, & l = j \\ -\text{sign}\{\mathcal{Q}_{jl}\} \times \pi/2 & l \neq j \end{cases}. \quad (37d)$$

In order to keep the amplitudes small, it is enough to take small reference amplitudes η_{jj} , since assuming $e^{2r} > |Q_{jj}|$, these are actually larger than the rest by a factor e^{2r} tops. On the other hand, the effective couplings (28) read in this case

$$\bar{g}_j = \frac{\eta_{jj}}{\sqrt{\cosh^2 r + e^{-2r} Q_{jj}^2/4}} g. \tag{38}$$

The effective couplings decrease then exponentially with the squeezing parameter r .

5. Example 2: continuous-variable GHZ states

5.1. GHZ states

As a second example we next consider the generation of continuous-variable GHZ states of different number of modes N [2, 37, 38]. In the unphysical limit of perfect entanglement, these states converge to the pure unnormalizable one $\int_{\mathbb{R}} dx \otimes_{j=1}^N |x\rangle$, where $|x\rangle$ are the eigenstates of the position quadratures \hat{x}_j . The most characteristic feature of this state is that it shows perfect correlation between all positions, as well as a well-defined center-of-mass momentum, since it is an eigenstate of the operators $\{\hat{x}_j - \hat{x}_i\}_{j=1, \dots, N}$ and $\sum_{j=1}^N \hat{p}_j$ with zero eigenvalue. It is common to summarize these correlations through the variances

$$\text{var} \left(\frac{\hat{x}_1 - \hat{x}_2}{\sqrt{2}} \right) = \text{var} \left(\frac{\hat{x}_2 - \hat{x}_3}{\sqrt{2}} \right) = \dots = \text{var} \left(\frac{\hat{x}_{N-1} - \hat{x}_N}{\sqrt{2}} \right) = \text{var} \left(\frac{\hat{p}_1 + \hat{p}_2 + \dots + \hat{p}_N}{\sqrt{N}} \right) = 0. \tag{39}$$

Remarkably, tracing out any of the modes turns the state of the remaining modes into the completely separable one $\int_{\mathbb{R}} dx \otimes_{j=1}^{N-1} |x\rangle \langle x|$, showing that this is a state with genuine multipartite entanglement. Note that for $N = 2$, this is just the well known EPR or two-mode perfectly-squeezed vacuum state [2, 30–33].

While this state is unphysical, one can easily build physical ones having the same qualitative properties [2, 37, 38]. For this, we just relax the perfect-correlation condition (39) as

$$\text{var} \left(\frac{\hat{p}_1 + \hat{p}_2 + \dots + \hat{p}_N}{\sqrt{N}} \right) = e^{-2r_1}, \tag{40a}$$

$$\text{var} \left(\frac{\hat{x}_1 - \hat{x}_2}{\sqrt{2}} \right) = \text{var} \left(\frac{\hat{x}_2 - \hat{x}_3}{\sqrt{2}} \right) = \dots = \text{var} \left(\frac{\hat{x}_{N-1} - \hat{x}_N}{\sqrt{2}} \right) = e^{-2r_2}, \tag{40b}$$

for some finite real and positive parameters r_1 and r_2 . Now the correlations are not perfect, but are still well beyond those of coherent-state mixtures (for which the previous variances are lower bounded by 1), so the states are nonclassical. States satisfying (40) can be built in a very neat way by starting with N single-mode squeezed states ($N - 1$ in position and 1 in momentum) and mixing them in a succession of beam-splitters for neighboring modes [2, 37, 38]. In particular, consider the following state

$$|\psi(r_1, r_2)\rangle = \underbrace{\hat{B}_{N-1, N}(\theta_{N-1}) \dots \hat{B}_{23}(\theta_2) \hat{B}_{12}(\theta_1) \hat{S}_N(-r_2) \dots \hat{S}_2(-r_2) \hat{S}_1(r_1)}_{\hat{G}} |vac\rangle_a, \tag{41}$$

with

$$\hat{B}_{jl}(\theta) = e^{\theta(\hat{a}_j \hat{a}_l^\dagger - \hat{a}_j^\dagger \hat{a}_l)} e^{i\pi \hat{a}_l^\dagger \hat{a}_l} \implies \begin{cases} \hat{B}_{jl}^\dagger(\theta) \hat{a}_j \hat{B}_{jl}(\theta) = \hat{a}_j \cos \theta + \hat{a}_l \sin \theta \\ \hat{B}_{jl}^\dagger(\theta) \hat{a}_l \hat{B}_{jl}(\theta) = -\hat{a}_l \cos \theta + \hat{a}_j \sin \theta \end{cases}, \tag{42}$$

and beam-splitter angles given by

$$\cos \theta_n = \frac{1}{\sqrt{N - n + 1}}, \quad \sin \theta_n = \sqrt{\frac{N - n}{N - n + 1}}. \tag{43}$$

The GHZ state (41) is already written as the action of a Gaussian unitary \hat{G} on the vacuum of the original modes as in (5). Moreover, we know from (32) and (42) how each of the unitaries act as a linear operation on the annihilation and creation operators:

$$\hat{S}_j^\dagger(r) \hat{\alpha} \hat{S}_j(r) = \mathcal{S}_j(r) \hat{\alpha}, \quad \hat{B}_{jl}^\dagger(\theta) \hat{\alpha} \hat{B}_{jl}(\theta) = \mathcal{B}_{jl}(\theta) \hat{\alpha}. \tag{44}$$

Here $\mathcal{S}_j(r)$ is a matrix equal to the $2N \times 2N$ identity, except for entries $\cosh r$ at elements (j, j) and $(N + j, N + j)$, and entries $\sinh r$ at elements $(j, N + j)$ and $(N + j, j)$. On the other hand, $\mathcal{B}_{jl}(\theta)$ is also a

matrix equal to the $2N \times 2N$ identity, except for entries $\cos \theta$ at elements (j, j) and $(N + j, N + j)$, entries $-\cos \theta$ at elements (l, l) and $(N + l, N + l)$, and entries $\sin \theta$ at elements (j, l) , (l, j) , $(N + j, N + l)$, and $(N + l, N + j)$. Hence, combining the action of all unitaries we find $\hat{G}^\dagger \hat{\alpha} \hat{G} = \mathcal{G} \hat{\alpha}$, with a matrix

$$\mathcal{G} = \mathcal{B}_{N-1,N}(\theta_{N-1}) \dots \mathcal{B}_{23}(\theta_2) \mathcal{B}_{12}(\theta_1) \mathcal{S}_N(-r_2) \dots \mathcal{S}_2(-r_2) \mathcal{S}_1(r_1) \equiv \begin{pmatrix} \mathcal{A} & \mathcal{B} \\ \mathcal{B}^* & \mathcal{A}^* \end{pmatrix}, \quad (45)$$

whose upper-left and upper-right blocks correspond to the matrices \mathcal{A} and \mathcal{B} that define the \hat{A} operators in (3).

In order to check that this construction leads to the desired GHZ state with correlations (40), we can evaluate the covariance matrix of the state (41) using (10). One can easily check (better with the help of some symbolic program to handle the matrix multiplications and diagonalization) that the covariance matrix has eigenvalues $e^{\pm 2r_1}$ and $e^{\pm 2r_2}$, the latter with $N - 1$ degeneracy. The corresponding eigenvectors are $(0, 0, \dots, 0, 1, 1, \dots, 1)^T$ for e^{-2r_1} and $\{(1, -1, 0, \dots, 0)^T, (0, 1, -1, 0, \dots, 0)^T, \dots, (0, \dots, 1, -1, 0, \dots, 0)\}^T$ for e^{-2r_2} , which correspond precisely to the desired quadratures when multiplied by \hat{r} .

5.2. Generation of GHZ states with our scheme

Let us now find the modulation amplitudes η_{jm} and phases ϕ_{jm} , equations (27) and (25), that lead to GHZ states in our scheme. We choose in this case $l_j = 1 \forall j$, that is, we take the modulation amplitudes $\{\eta_{jl}\}_{j=1,2,\dots,N}$ as the ones we control (this choice simply leads to more manageable expressions, but any other choice would lead to the same conclusions). Using the matrices \mathcal{A} and \mathcal{B} built as explained above for the GHZ state, it is not difficult to find by inspecting different N vales the following forms for the amplitudes and phases for arbitrary number of modes

$$\eta_{jl} = \eta_{jl} \times \begin{cases} 1, & l = 1 \\ 0, & l > j + 1 \\ \sqrt{\frac{N(N-j)}{N-j+1}} \frac{\cosh r_2}{\cosh r_1}, & l = j + 1 \\ \sqrt{\frac{N}{(N-l+2)(N-l+1)}} \frac{\cosh r_2}{\cosh r_1}, & 1 < l < j + 1 \end{cases}, \quad (46a)$$

$$\eta_{j,N+l} = \eta_{jl} \times \begin{cases} \tanh r_1 & l = 1 \\ \tanh r_2 & l > 1 \end{cases}, \quad (46b)$$

$$\phi_{jl} = \begin{cases} \pi, & l = 1 \text{ or } l > j \\ 0 & \text{otherwise} \end{cases}, \quad (46c)$$

$$\phi_{j,N+l} = \begin{cases} \pi, & l = j + 1 \\ 0 & \text{otherwise} \end{cases}, \quad (46d)$$

where in these expressions $j, l = 1, 2, \dots, N$. There are several notable things to mention here. First, assuming that we take all η_{jl} of the same order, say $\eta_{jl} = \eta \forall j$, note that the largest amplitude is $\eta_{12} = \sqrt{N-1} \eta$ (further assuming $r_1 = r_2$ for simplicity), which we need to make sure stays much smaller than 1, e.g. we need to choose $\eta = 0.1/\sqrt{N-1}$. On the other hand, particularized to the GHZ state, (28) leads to the effective couplings

$$\bar{g}_j = \frac{\sqrt{N} \eta_{j1}}{\cosh r_1} g. \quad (47)$$

Remarkably, the effective couplings do not depend on r_2 , but decrease exponentially with r_1 . Also, they are dressed by a factor \sqrt{N} , so they do not ‘feel’ the $1/\sqrt{N-1}$ reduction of η mentioned above. In other words, the cooling rates are approximately independent of N , similarly to what we found for cluster states.

6. Limits imposed by the $|n| = 3$ resonances

With the examples at hand, we can now give more quantitative details about the error that one would make when not considering higher η -order resonances, in particular those occurring at $|n| = 3$. In order to do this, we can simply compute the fidelity or overlap between the states with and without the correction given in (29).

Let us denote by $\tilde{\mathcal{A}}$ and $\tilde{\mathcal{B}}$ the matrices of the Gaussian state including the correction. The interaction-picture Hamiltonian (18) still has the form of the effective Hamiltonian (13), $\sum_{j=1}^N \tilde{g}_j \hat{\sigma}_j [\sum_{l=1}^N (\tilde{\mathcal{A}}_{jl} \hat{a}_l + \tilde{\mathcal{B}}_{jl} \hat{a}_l^\dagger)] + \text{H.c.}$, but now with the correspondences $\tilde{g}_j \tilde{\mathcal{A}}_{jl} = -g \alpha_{jl}$ and $\tilde{g}_j \tilde{\mathcal{B}}_{jl} = -g \beta_{jl}$,

with α_{ji} and β_{ji} expressed to third order in the modulation amplitudes η_{jm} as given by (29). The qubits will now cool the modes to the ground state of a Gaussian state with modified matrices and effective couplings, as given by

$$\tilde{g}_j = g \sqrt{\sum_{k=1}^N (|\alpha_{jk}|^2 - |\beta_{jk}|^2)}, \quad \tilde{\mathcal{A}}_{jl} = -\frac{\alpha_{jl}}{\sqrt{\sum_{k=1}^N (|\alpha_{jk}|^2 - |\beta_{jk}|^2)}}, \quad \tilde{\mathcal{B}}_{jl} = -\frac{\beta_{jl}}{\sqrt{\sum_{k=1}^N (|\alpha_{jk}|^2 - |\beta_{jk}|^2)}}, \quad (48)$$

where the modulation amplitudes η_{jm} and phases ϕ_{jm} are chosen as (46) for the cluster state example or (46) for the GHZ example. Given these expressions and using (7), we can then build the covariance matrix of the modified Gaussian state as

$$\tilde{V} = \mathcal{T} \begin{pmatrix} \tilde{\mathcal{A}}\tilde{\mathcal{B}}^T & \tilde{\mathcal{A}}\tilde{\mathcal{A}}^\dagger \\ \tilde{\mathcal{B}}^*\tilde{\mathcal{B}}^T & \tilde{\mathcal{B}}^*\tilde{\mathcal{A}}^\dagger \end{pmatrix} \mathcal{T}^T - i\mathcal{W}. \quad (49)$$

Now all that is left is comparing the ideal Gaussian state $|\psi\rangle$ with covariance matrix (10) and this modified one, that we denote by $|\tilde{\psi}\rangle$. We denote the corresponding Wigner functions by $W(\mathbf{r})$ and $\tilde{W}(\mathbf{r})$, which are Gaussians of zero mean in both cases. Now, since they are pure states, we compare them through the overlap, which is easily evaluated as [2, 30–33]

$$\begin{aligned} |\langle\psi|\tilde{\psi}\rangle|^2 &= (4\pi)^N \int_{\mathbb{R}^{2N}} d^{2N}\mathbf{r} W(\mathbf{r}) \tilde{W}(\mathbf{r}) \\ &= \frac{(4\pi)^N}{(2\pi)^{2N} \sqrt{\det\{V\} \det\{\tilde{V}\}}} \int_{\mathbb{R}^{2N}} d^{2N}\mathbf{r} e^{-\frac{1}{2}\mathbf{r}^T (V^{-1} + \tilde{V}^{-1})\mathbf{r}} = \frac{2^N}{\sqrt{\det\{V^{-1} + \tilde{V}^{-1}\}}}, \end{aligned} \quad (50)$$

where we have used $\det\{V\} = 1 = \det\{\tilde{V}\}$ since the states are pure.

In the case of cluster states, we have examined the fidelity for up to $N = 50$ modes and many random instances of the matrix \mathcal{Q} with elements in the interval $[-4, 4]$ different geometries for the connections between pairs of modes. Taking the reference amplitudes $\eta_{ij} = 0.1$, we have never found an instance with overlap smaller than 0.95, even for 99% squeezing ($e^{-2r_1} = e^{-2r_2} = 0.1$).

As for GHZ states, they show a bit more sensitivity to these corrections. Setting the reference amplitudes to $\eta_{ij} = 0.1/\sqrt{N-1}$, for 90% squeezing ($e^{-2r_1} = e^{-2r_2} = 0.1$) we have checked that the fidelity remains above 0.998 for as large N as we have been patient enough to compute ($N = 10$). For $N = 10$, we have seen that the fidelity falls below 0.99, 0.95, and 0.9 only if the squeezing exceeds, respectively, 95.1%, 97.7%, and 98.3% ($e^{-2r_1} = e^{-2r_2} = 0.049, 0.023, \text{ and } 0.017$).

For both types of states we have checked that the effective couplings \tilde{g}_j remain extremely close to the original ones \bar{g}_j (say, within 5 significant digits) for the largest squeezing and number of modes that we have computed.

7. Avoiding all-to-all coupling

Perhaps the main experimental hurdle of our proposal is the fact that the model we present has connections of all modes to all qubits, which is pretty unrealistic through direct coupling in current architectures. Fortunately, effective ways such as those relying on resonator networks can help [39]. As a proof of concept, we consider here a simpler situation: we next show that a chain of nearest-neighbor-coupled modes, with each mode locally coupled to a single qubit, achieves the type of Hamiltonian we need in the normal-mode basis of the chain. We compare two types of chains that allow us for analytic calculations: one with open boundaries and one with closed boundaries.

7.1. Open bosonic chain

Consider first the model

$$\hat{H} = \sum_{j=1}^{N-1} \left(\omega \hat{a}_j^\dagger \hat{a}_j - J \hat{a}_j \hat{a}_{j+1}^\dagger - J \hat{a}_j^\dagger \hat{a}_{j+1} + \frac{\varepsilon_j}{2} \hat{\sigma}_j^z \right) + \sum_{j=1}^N g_j (\hat{\sigma}_j + \hat{\sigma}_j^\dagger) (\hat{a}_j + \hat{a}_j^\dagger). \quad (51)$$

We have taken all the mode frequencies and hoppings equal (homogeneous chain) in order to be able to perform analytic calculations. We can move to a normal-mode basis that diagonalizes the bosonic part of this model, which we write as $\hat{\mathbf{a}}^\dagger \mathcal{M} \hat{\mathbf{a}}$, with a tridiagonal matrix

where the only difference with the all-to-all connected model is that the target matrices are \mathcal{S} -transformed, $\mathcal{A}^{(c)}$ and $\mathcal{B}^{(c)}$, and the modulation phases need to cancel additional phases (signs) coming from some of the $\sin(\frac{k_j\pi}{N+1})$ terms in the couplings g_{jk} . Specifically, assuming couplings $g_{jk} = g \sin(\frac{k_j\pi}{N+1})$ of equal magnitude except for the sinusoidal modulation, we can make the same choices as we did in equations (25) and (27):

$$\eta_{jk} = \left| \frac{\mathcal{A}_{jk}^{(c)} \sin\left(\frac{\bar{k}_j\pi}{N+1}\right)}{\mathcal{A}_{\bar{j}_j}^{(c)} \sin\left(\frac{k_j\pi}{N+1}\right)} \right| \eta_{\bar{j}_j}, \tag{58a}$$

$$\eta_{j,N+k} = \left| \frac{\mathcal{B}_{jk}^{(c)} \sin\left(\frac{\bar{k}_j\pi}{N+1}\right)}{\mathcal{A}_{\bar{j}_j}^{(c)} \sin\left(\frac{k_j\pi}{N+1}\right)} \right| \eta_{\bar{j}_j}, \tag{58b}$$

$$\phi_{jk} = \arg\left\{ \sin\left(\frac{k_j\pi}{N+1}\right) \right\} - \arg\{\mathcal{A}_{jk}^{(c)}\}, \tag{58c}$$

$$\phi_{j,N+k} = \arg\left\{ \sin\left(\frac{k_j\pi}{N+1}\right) \right\} - \arg\{\mathcal{B}_{jk}^{(c)}\}, \tag{58d}$$

where the reference amplitudes $\{\eta_{\bar{j}_j}\}_{j=1,2,\dots,N}$ are fixed to whatever value we want, and the effective couplings read

$$\bar{g}_j = g \eta_{\bar{j}_j} \left| \frac{\sin\left(\frac{\bar{k}_j\pi}{N+1}\right)}{\mathcal{A}_{\bar{j}_j}^{(c)}} \right|. \tag{59}$$

7.2. Closed bosonic chain

Consider next the model

$$\hat{H} = \sum_{j=1}^N \left(\omega \hat{a}_j^\dagger \hat{a}_j - J e^{i\phi} \hat{a}_j \hat{a}_{j+1}^\dagger - J e^{-i\phi} \hat{a}_j^\dagger \hat{a}_{j+1} + \frac{\epsilon_j}{2} \hat{\sigma}_j^z \right) + \sum_{j=1}^N g_j (\hat{\sigma}_j + \hat{\sigma}_j^\dagger) (\hat{a}_j + \hat{a}_j^\dagger). \tag{60}$$

where again we take all the mode frequencies and hoppings equal (homogeneous chain) in order to be able to perform analytic calculations. We will see in a second that this forces us to introduce complex hoppings $\phi \neq 0$ (sometimes referred to as ‘external artificial Gauge field’) for our ideas to work, but real hoppings would work as well as long as the chain is sufficiently inhomogeneous. Periodic boundaries are assumed this time, that is, $\hat{a}_{N+1} \equiv \hat{a}_1$. Let’s move to the Fourier basis that diagonalizes the bosonic part of this model

$$\hat{a}_j = \frac{1}{\sqrt{N}} \sum_{k=k_{\min}}^{k_{\min}+N-1} e^{2\pi ijk/N} \hat{c}_k \iff \hat{c}_k = \frac{1}{\sqrt{N}} \sum_{j=1}^N e^{-2\pi ijk/N} \hat{a}_j, \tag{61}$$

where we choose to work in the first Brillouin zone so that $k_{\min} = -N/2$ or $-(N-1)/2$ for even or odd N , respectively. Inserting this expression in (60) and using the completeness relation $\sum_{j=1}^N e^{2\pi ij(k-k')/N} = N\delta_{k,k'}$, we easily obtain

$$\hat{H} = \sum_{k=k_{\min}}^{k_{\min}+N-1} \Delta_k \hat{c}_k^\dagger \hat{c}_k + \sum_{j=1}^N \frac{\epsilon_j}{2} \hat{\sigma}_j^z + \sum_{j=1}^N \sum_{k=k_{\min}}^{k_{\min}+N-1} (\hat{\sigma}_j + \hat{\sigma}_j^\dagger) (g_{jk} \hat{c}_k + g_{jk}^* \hat{c}_k^\dagger), \tag{62}$$

where we have defined the dispersion relation $\Delta_k = \omega - 2J \cos(2\pi k/N - \phi)$ and the complex couplings $g_{jk} = e^{2\pi ijk/N} g_j / \sqrt{N}$. The couplings are now reduced by a \sqrt{N} factor, but do not possess the sinusoidal modulation present in the open chain, so in this case there is no restriction on the values of N . Importantly, the condition that all mode frequencies must be different, $\Delta_k \neq \Delta_{k' \neq k}$, imposes that ϕ cannot take certain values such as 0 or π , for which $\Delta_k = \Delta_{-k}$. Hence, having complex hopping in the homogeneous chain is a necessary condition. Of course, it might be experimentally easier to work with an inhomogeneous chain (e.g. bosonic modes of unequal frequencies) and keep the hoppings real. Also, note that as N increases, the difference between Δ_k and $\Delta_{k\pm 1}$ decreases; we can estimate the worst case situation in the same way as we did above for the open chain, by considering in this case a mode k at the bottom of the dispersion relation and a neighboring one, whose difference is given by $2J[1 - \cos(2\pi/N)] \approx 8\pi^2 J/N^2$ for large N , showing that if we want to keep this difference on the order of the largest coupling $\max(|g_j|/\sqrt{N}) \equiv g$, the hopping will have to scale again as the square of the number of modes, that is, $J \geq gN^2/8\pi^2$. Taking $g = 2\pi \times 40$ MHz, we

apply again the condition that the smallest qubit frequency $\varepsilon_N = 2\pi \times 10 \text{ GHz} - (N-1)g$ must be larger than the largest Fourier-mode frequency $\omega_{\max} \leq 2\pi \times 1 \text{ GHz} + 4J \sim 2\pi \times 1 \text{ GHz} + gN^2/2\pi^2$, obtaining $\varepsilon_N - \omega_{\max} > 50g$ as long as $N < 50$, which is again a large number of modes.

We finally need to consider again the state to which we need to cool down the Fourier modes in order to obtain a desired Gaussian state of the original modes. The relation between these modes can be written now as $\hat{\mathbf{a}} = \mathcal{F}\hat{\mathbf{c}}$, with \mathcal{F} a unitary matrix with elements $\mathcal{F}_{jk} = e^{2\pi ijk/N}/\sqrt{N}$ and $\hat{\mathbf{c}} = (\hat{c}_{k_{\min}}, \hat{c}_{k_{\min}+1}, \dots, \hat{c}_{k_{\min}+N-1})^T$ collecting all the Fourier annihilation operators. Then, applying \mathcal{F}^\dagger on (3), we obtain the action of the Gaussian unitary \hat{G} that defines the target state $|G\rangle = \hat{G}|\text{vac}\rangle_a$ on the Fourier modes, which defines the new set of bosonic operators $\hat{\mathbf{C}}$ that we will need to cool down:

$$\hat{G}^\dagger \hat{\mathbf{c}} \hat{G} = \underbrace{\mathcal{F}^\dagger \mathcal{A} \mathcal{F}}_{\mathcal{A}^{(c)}} \hat{\mathbf{c}} + \underbrace{\mathcal{F}^\dagger \mathcal{B} \mathcal{F}^*}_{\mathcal{B}^{(c)}} \hat{\mathbf{c}}^\dagger \equiv \hat{\mathbf{C}}. \quad (63)$$

The qubit modulation

$$\sum_{j=1}^N \left[\sum_{k=k_{\min}}^{k_{\min}+2N-1} \Omega_{jk} \eta_{jk} \cos(\Omega_{jk}t + \phi_{jk}) \right] \hat{\sigma}_j^z \quad (64)$$

would now induce the effective Hamiltonian

$$\hat{H}_{\text{eff}} = - \sum_{j=1}^N \bar{g}_j \hat{\mathbf{C}}_j \hat{\sigma}_j^\dagger + \text{H.c.}, \quad (65)$$

as long as the modulation amplitudes and phases are chosen to satisfy

$$\bar{g}_j \mathcal{A}_{jk}^{(c)} = g_{jk} \eta_{jk} e^{-i\phi_{jk}}, \quad \bar{g}_j \mathcal{B}_{jk}^{(c)} = g_{jk}^* \eta_{j,N+k} e^{-i\phi_{j,N+k}}. \quad (66)$$

Assuming couplings $g_{jk} = g \exp(2\pi ijk/N)$ of equal magnitude, we can make the same choices as we did in previous sections, equations (27) and (25):

$$\eta_{jk} = \frac{|\mathcal{A}_{jk}^{(c)}|}{|\mathcal{A}_{j\bar{k}_j}^{(c)}|} \eta_{j\bar{k}_j}, \quad \eta_{j,N+k} = \frac{|\mathcal{B}_{jk}^{(c)}|}{|\mathcal{A}_{j\bar{k}_j}^{(c)}|} \eta_{j\bar{k}_j}, \quad (67a)$$

$$\phi_{jk} = 2\pi \frac{jk}{N} - \arg\{\mathcal{A}_{jk}^{(c)}\}, \quad \phi_{j,N+k} = -2\pi \frac{jk}{N} - \arg\{\mathcal{B}_{jk}^{(c)}\}, \quad (67b)$$

where $\{\eta_{j\bar{k}_j}\}_{j=1,2,\dots,N}$ are fixed to whatever value we want as usual, and the effective couplings read

$$\bar{g}_j = g \frac{\eta_{j\bar{k}_j}}{|\mathcal{A}_{j\bar{k}_j}^{(c)}|}. \quad (68)$$

8. Concluding remarks

We have shown how to modulate a collection of lossy qubits coupled to a set of bosonic modes so as to dissipatively steer the latter into any desired multimode Gaussian state. While we have initially presented the idea for an all-to-all coupling geometry (cleaner for the theoretical analysis), we have also proven that it can be avoided by, for example, using a bosonic chain with local couplings to the qubits, which looks experimentally friendlier. We have explicitly shown how to modulate the qubits so as to generate two paradigmatic families of states: cluster and GHZ states. These examples have proven that the modulation amplitudes η_{jm} and effective couplings \bar{g}_j have similar parametric dependences on the relevant physical parameters as their counterparts in our previous single-mode work [29]. The only potential issue we need to be careful with is choosing the qubit and mode frequencies such that there are no higher η -order resonances, to which the multimode protocol is more prone to. Essentially, this just requires that all frequency differences are large enough with respect to the couplings g . Taking $g/2\pi = 40 \text{ MHz}$ as in the previous sections, with $\varepsilon_1/2\pi = 10 \text{ GHz}$, $\omega_1/2\pi = 4.8 \text{ GHz}$, and the rest of frequencies equally spaced as $\{\varepsilon_{j+1} = \varepsilon_1 - 10gj, \omega_{j+1} = \omega_1 - 10gj\}_{j=1,2,\dots,N-1}$, we can reach $N = 10$ while still keeping the lowest frequency above 1 GHz, which is reasonable for superconducting circuits. Of course, way larger N can be obtained by decreasing the spacing between modes, and we have indeed checked that even taking $|\omega_j - \omega_{j+1}| = g$ we can still satisfy the conditions required for α_{jl} and β_{jl} to not receive relevant higher η -order contributions while reaching $N > 100$.

Regarding the dissipative preparation of the Gaussian state through cooling, let us refer to the effective master equation (14) of the bosonic modes after adiabatic elimination of the qubits. The effective removal of bosonic excitations requires very lossy qubits, say with spontaneous emission rate $\gamma_j/2\pi = 400$ MHz ten times larger than the coupling g . On the other hand, bosonic excitations should not decay through their own natural environment, and thus high-quality bosonic modes are required. Let us take $\kappa/2\pi = 1$ KHz, accessible in superconducting devices where extremely high quality factors have been realized. These parameters allow reaching large cooperativities on the order of $\bar{g}_j^2/\gamma_j\kappa \sim g^2\eta^2/\gamma_j\kappa \cosh^2 r \approx 13$ for modulation amplitudes $\eta \approx 0.1$ and 90%-squeezing levels ($e^{-2r} \approx 0.1$), where we have used the effective couplings $\bar{g}_j \sim g\eta/\cosh r$ derived from the examples. For this value of the cooperativity one expects just a small mixed correction to the ideal Gaussian pure state, similarly to what we found in [29].

Let us remark that once we know how to generate arbitrary Gaussian states through cooling, we can also do it via lasing, just adapting the ideas we presented in [29]. In particular, one would need to add an auxiliary set of qubits, but modulated in such a way that the anti-Jaynes–Cummings equivalent of (13) is generated, that is, an effective Hamiltonian of the form $-\sum_{j=1}^N \bar{g}_j (\hat{A}_j \hat{\sigma}_j + \hat{A}_j^\dagger \hat{\sigma}_j^\dagger)$. In order to accomplish this, one just needs to replace the correspondence (24b) by

$$\bar{g}_j \hat{A}_j^\dagger = \sum_{l=1}^N g_{jl} \left(\eta_{jl} e^{-i\phi_{jl}} \hat{a}_l + \eta_{j,N+l} e^{-i\phi_{j,N+l}} \hat{a}_l^\dagger \right) \quad (69a)$$

$$\bar{g}_j \mathcal{B}_{jl}^* = g_{jl} \eta_{jl} e^{-i\phi_{jl}}, \quad \bar{g}_j \mathcal{A}_{jl}^* = g_{jl} \eta_{j,N+l} e^{-i\phi_{j,N+l}}, \quad j, l = 1, 2, \dots, N. \quad (69b)$$

After tracing out the qubits used for cooling, one is then left with the following master equation for the state $\hat{\rho}$ of the bosonic modes and the auxiliary qubits [29]:

$$\frac{d\hat{\rho}}{dt} = \sum_{j=1}^N \left(i\bar{g}_j \left[\hat{A}_j \hat{\sigma}_j + \hat{A}_j^\dagger \hat{\sigma}_j^\dagger, \hat{\rho} \right] + \mathcal{D}_{A_j}[\hat{\rho}] + \mathcal{D}_{\sigma_j}[\hat{\rho}] \right). \quad (70)$$

This is equivalent to the master equation of a collection of independent single-qubit lasers [29] for each bosonic mode \hat{A}_j (note that exchanging the dummy labels between the qubit states, $|g\rangle_j \rightleftharpoons |e\rangle_j$, is equivalent to a $\hat{\sigma}_j \rightleftharpoons \hat{\sigma}_j^\dagger$ swap, turning the qubit dissipation into pumping, and the Hamiltonian into a Jaynes–Cummings one). This opens the possibility of experimentally engineering nonclassical multimode lasing, something that sounds quite exotic specially in the context of optical settings.

Data availability statement

No new data were created or analysed in this study.

Acknowledgments

CNB thanks Valentina Hopekin for inspiration with the manuscript, and acknowledges sponsorship from the Yangyang Development Fund, as well as support from a Shanghai talent program and from the Shanghai Municipal Science and Technology Major Project (Grant No. 2019SHZDZX01). DP and JJGR acknowledge financial support from the Proyecto Sinérgico CAM 2020 Y2020/TCS-6545 (NanoQuCoCM), the CSIC Interdisciplinary Thematic Platform (PTI+) on Quantum Technologies (PTI-QTEP+) and from Spanish Project PID2021-127968NB-I00 (MCIU/AEI/FEDER, EU).

ORCID iDs

Juan José García-Ripoll  <https://orcid.org/0000-0001-8993-4624>

Diego Porras  <https://orcid.org/0000-0003-2995-0299>

References

- [1] Fabre C and Treps N 2020 *Rev. Mod. Phys.* **92** 035005
- [2] Braunstein S L and van Loock P 2005 *Rev. Mod. Phys.* **77** 513
- [3] Raussendorf R and Briegel H J 2001 *Phys. Rev. Lett.* **86** 5188
- [4] Menicucci N C, van Loock P, Gu M, Weedbrook C, Ralph T C and Nielsen M A 2006 *Phys. Rev. Lett.* **97** 110501
- [5] Menicucci N C, Flammia S T and Pfister O 2008 *Phys. Rev. Lett.* **101** 130501
- [6] Armstrong S, Morizur J-F, Janousek J, Hage B, Treps N, Lam P K and Bachor H-A 2012 *Nat. Commun.* **3** 1026
- [7] Chen M, Menicucci N C and Pfister O 2014 *Phys. Rev. Lett.* **112** 120505

- [8] Gerke S, Sperling J, Vogel W, Cai Y, Roslund J, Treps N and Fabre C 2015 *Phys. Rev. Lett.* **114** 050501
- [9] Larsen M V, Guo X, Breum C R, Neergaard-Nielsen J S and Andersen U L 2019 *Science* **366** 369
- [10] Asavanant W et al 2019 *Science* **366** 373
- [11] Wang W, Zhang K and Jing J 2020 *Phys. Rev. Lett.* **125** 140501
- [12] Zhong H-S et al 2020 *Science* **370** 1460
- [13] Larsen M V, Guo X, Breum C R, Neergaard-Nielsen J S and Andersen U L 2021 *Nat. Phys.* **17** 1018
- [14] Madsen L S et al 2022 *Nature* **606** 75
- [15] García-Ripoll J J 2022 *Quantum Information and Quantum Optics with Superconducting Circuits* (Cambridge University Press)
- [16] Blais A, Grimsmo A L, Girvin S M and Wallraff A 2021 *Rev. Mod. Phys.* **93** 025005
- [17] Devoret M H and Schoelkopf R J 2013 *Science* **339** 1169
- [18] Arute F et al 2019 *Nature* **574** 505
- [19] Morvan A et al 2023 Phase transition in random circuit sampling (arXiv:2304.11119)
- [20] Gong M et al 2023 *Sci. Bull.* **68** 906
- [21] Wu Y et al 2021 *Phys. Rev. Lett.* **127** 180501
- [22] Forn-Díaz P, Lisenfeld J, Marcos D, García-Ripoll J J, Solano E, Harmans C J P M and Mooij J E 2010 *Phys. Rev. Lett.* **105** 237001
- [23] Niemczyk T et al 2010 *Nat. Phys.* **6** 772
- [24] Yoshihara F, Fuse T, Ashhab S, Kakuyanagi K, Saito S and Semba K 2017 *Nat. Phys.* **13** 44
- [25] Forn-Díaz P, García-Ripoll J J, Peropadre B, Orgiazzi J-L, Yurtalan M, Belyansky R, Wilson C and Lupascu A 2017 *Nat. Phys.* **13** 39
- [26] Li J et al 2013 *Nat. Commun.* **4** 1420
- [27] Lähteenmäki P, Paraoanu G S, Hassel J and Hakonen P J 2013 *Proc. Natl Acad. Sci.* **110** 4234
- [28] Porras D and García-Ripoll J J 2012 *Phys. Rev. Lett.* **108** 043602
- [29] Navarrete-Benlloch C, García-Ripoll J J and Porras D 2014 *Phys. Rev. Lett.* **113** 193601
- [30] Navarrete-Benlloch C 2015 *An Introduction to the Formalism of Quantum Information with Continuous Variables* (Morgan & Claypool and IOP)
- [31] Weedbrook C, Pirandola S, García-Patrón R, Cerf N J, Ralph T C, Shapiro J H and Lloyd S 2012 *Rev. Mod. Phys.* **84** 621
- [32] Ferraro A, Olivares S and Paris M G A 2005 *Gaussian States in Quantum Information* (Bibliopolis)
- [33] Navarrete-Benlloch C 2022 Introduction to quantum optics (arXiv:2203.13206)
- [34] Zhang J and Braunstein S L 2006 *Phys. Rev. A* **73** 032318
- [35] Menicucci N C, Flammia S T and van Loock P 2011 *Phys. Rev. A* **83** 042335
- [36] Carmichael H J 1999 *Statistical Methods in Quantum Optics 1: Master Equations and Fokker-Planck Equations* (Springer)
- [37] van Loock P and Braunstein S L 2000 *Phys. Rev. Lett.* **84** 3482
- [38] van Loock P and Furusawa A 2003 *Phys. Rev. A* **67** 052315
- [39] Olivares D G, Peropadre B, Huh J and García-Ripoll J J 2017 *Phys. Rev. Appl.* **8** 064008
- [40] Noschese S, Pasquini L and Reichel L 2013 *Numer. Linear Algebra Appl.* **20** 302